

Piezoelectric and Electromechanical Characteristics of Porous Poly(Ethylene-co-Vinyl Acetate) Copolymer Films for Smart Sensors and Mechanical Energy Harvesting Applications

Chouaib Ennawaoui, Abdelowahed Hajjaji, Cédric Samuel, Erroumayssae Sabani, Abdelkader Rjafallah, Ikrame Najihi, El Mehdi Laadissi, El Mehdi Loualid, Mohamed Rguiti, Abdessamad El Ballouti, et al.

▶ **To cite this version:**

Chouaib Ennawaoui, Abdelowahed Hajjaji, Cédric Samuel, Erroumayssae Sabani, Abdelkader Rjafallah, et al.. Piezoelectric and Electromechanical Characteristics of Porous Poly(Ethylene-co-Vinyl Acetate) Copolymer Films for Smart Sensors and Mechanical Energy Harvesting Applications. Applied System Innovation, 2021, 4 (3), pp.57. 10.3390/asi4030057 . hal-03703173

HAL Id: hal-03703173
https://uphf.hal.science/hal-03703173

Submitted on 6 Jul 2022

HAL is a multi-disciplinary open access archive for the deposit and dissemination of scientific research documents, whether they are published or not. The documents may come from teaching and research institutions in France or abroad, or from public or private research centers.

L'archive ouverte pluridisciplinaire **HAL**, est destinée au dépôt et à la diffusion de documents scientifiques de niveau recherche, publiés ou non, émanant des établissements d'enseignement et de recherche français ou étrangers, des laboratoires publics ou privés.



Distributed under a Creative Commons Attribution| 4.0 International License

applied system innovation

MDPI

Article

Piezoelectric and Electromechanical Characteristics of Porous Poly(Ethylene-*co*-Vinyl Acetate) Copolymer Films for Smart Sensors and Mechanical Energy Harvesting Applications

Chouaib Ennawaoui [1,*], Abdelowahed Hajjaji [1], Cédric Samuel [2], Erroumayssae Sabani [1], Abdelkader Rjafallah [1], Ikrame Najihi [1], El Mehdi Laadissi [1], El Mehdi Loualid [1], Mohamed Rguiti [3], Abdessamad El Ballouti [1] and Azeddine Azim [1]

[1] Sciences Engineer Laboratory for Energy (LabSIPE), National School of Applied Sciences, Chouaïb Doukkali University, El Jadida 24030, Morocco; hajjaji12@gmail.com (A.H.); erroumayssae@gmail.com (E.S.); rjafallah.abdelkader@gmail.com (A.R.); najihi.ikram@gmail.com (I.N.); laadissi.e@ucd.ac.ma (E.M.L.); loualid.m@ucd.ac.ma (E.M.L.); elballouti@hotmail.com (A.E.B.); azim.a@ucd.ac.ma (A.A.)

[2] IMT Lille Douai, Institut Mines-Telecom, Univ. Lille, Centre for Materials and Processes, F-59000 Lille, France; cedric.samuel@imt-lille-douai.fr

[3] EA 2443-LMCPA-Laboratory of Ceramic Materials and Associated Processes, Polytechnic University of Hauts-de-France, F-59313 Valenciennes, France; mohamed.rguiti@uphf.fr

* Correspondence: chouaib.enna@gmail.com

Abstract: This paper investigates energy harvesting performances of porous piezoelectric polymer films to collect electrical energy from vibrations and power various sensors. The influence of void content on the elastic matrix, dielectric, electrical, and mechanical properties of porous piezoelectric polymer films produced from available commercial poly(ethylene-*co*-vinyl acetate) using an industrially applicable melt-state extrusion method (EVA) were examined and discussed. Electrical and mechanical characterization showed an increase in the harvested current and a decrease in Young's modulus with the increasing ratio of voids. Thermal analysis revealed a decrease in piezoelectric constant of the porous materials. The authors present a mathematical model that is able to predict harvested current as a function of matrix characteristics, mechanical excitation and porosity percentage. The output current is directly proportional to the porosity percentage. The harvested power significantly increases with increasing strain or porosity, achieving a power value up to 0.23, 1.55, and 3.87 mW/m^3 for three EVA compositions: EVA 0%, EVA 37% and EVA 65%, respectively. In conclusion, porous piezoelectric EVA films has great potential from an energy density viewpoint and could represent interesting candidates for energy harvesting applications. Our work contributes to the development of smart materials, with potential uses as innovative harvester systems of energy generated by different vibration sources such as roads, machines and oceans.

Keywords: porous polymers; piezoelectric effect; poly(ethylene-*co*-vinyl acetate); mechanical energy harvesting

check for updates

Citation: Ennawaoui, C.; Hajjaji, A.; Samuel, C.; Sabani, E.; Rjafallah, A.; Najihi, I.; Laadissi, E.M.; Loualid, E.M.; Rguiti, M.; Ballouti, A.E.; et al. Piezoelectric and Electromechanical Characteristics of Porous Poly(Ethylene-*co*-Vinyl Acetate) Copolymer Films for Smart Sensors and Mechanical Energy Harvesting Applications. *Appl. Syst. Innov.* **2021**, *4*, 57. https://doi.org/10.3390/asi4030057

Academic Editor: Andrey Chernov

Received: 14 July 2021
Accepted: 18 August 2021
Published: 26 August 2021

Publisher's Note: MDPI stays neutral with regard to jurisdictional claims in published maps and institutional affiliations.

Copyright: © 2021 by the authors. Licensee MDPI, Basel, Switzerland. This article is an open access article distributed under the terms and conditions of the Creative Commons Attribution (CC BY) license (https://creativecommons.org/licenses/by/4.0/).

1. Introduction

Piezoelectric materials are optimized for special applications ranging from mechanical structures to electronic devices, from applications in structural health monitoring and aerospace to active vibration damping and the automotive industry [1–4]. Today, piezoelectric polymers have been considered for energy harvesting applications [5–8]. The material has remarkable fatigue resistance and environmental stability [9], but it has not been recognized as a promising energy harvesting material because of its low piezoelectric constants when compared to PZT ceramics [10–12]. Recently, researchers investigated porous piezoelectric polymers consisting of an ionized cellular polypropylene film made by a chemical elaboration method using nitrogen gas [13]. Excellent piezoelectric coefficients up to 2000 pC/N for

specific morphologies and mechanical conditions comparably higher than those of piezoceramics were identified [14,15]. In order to demonstrate the ability of the porous piezoelectric polymers in a harsh environment, Zhong et al. [16] fabricated PET/EVA/PET laminated films and ionized them by a corona charging method. The longitudinal piezoelectric coefficient of the developed generator reached ~6300 pC/N. Zhang et al. [15] showed energy harvesting applications with this type of cellular material based on piezoelectret fluorocarbon polymers with a power collected value up to 109 W [16]. Kachroudi et al. [17] examined air-spaced cantilevers elaborated from a PDMS porous piezoelectric material for energy harvesting applications. For frequencies ranging from 5 Hz to 200 Hz, the output power reached a maximum of 136 nW and remained stable at 103 nW.

Different procedures, techniques and methods have been developed and used in order to prepare the porous polymers, e.g., compression molding [18], extrusion [19,20], injection [21], solvent casting [22], tape casting [23], and spin coating [24]. Void content creation techniques provide opportunities to fabricate advanced polymers with greater physical proprieties and controlled volume as a function of porosity fraction [25]. The porous piezoelectric ceramics mainly suffer from low mechanical proprieties, high cost for preparation and limited application fields [26]. Porous piezoelectric polymers can be described as particles that contain void or gas by a coating or shell and have diameters in the 1–1000 µm range [27]. Commercial uses for this type of material include functional textiles, adhesives, cosmetics, medicines, and other medical applications [28,29]. Physical methods, chemical methods, and physico-chemical methods are the three strategies used to create porous polymers [30–32]. The physical methods contain techniques such as spray cooling, spray drying and fluidized bed processes, and the chemical methods contain in situ polymerization and the solvent extraction/evaporation method. The physico-chemical methods contain simple and complex methods as well as sol gel technology. After the elaboration step of polymer foams, gas ionization is an important step to create the pseudo piezoelectric effect [33–37]. Starting with a polymer film with embedded air cells, internal charging of air can be carried out through electrical ionization [38]. When a large electric field is applied across the film, gas molecules in the cells become ionized and opposite charges are accelerated and implanted on each side of the cells, depending on the applied electric field direction [39–41]. Such artificially embedded dipoles respond externally to an applied electrical field or mechanical force similar to piezoelectric material [42]. Porous piezoelectric polymers are also extremely flexible, making them ideal candidates for mechanical energy harvesters [43]. In this field, commercially available poly(ethylene-*co*-vinyl acetate) (EVA) could be of great interest, with an intrinsic low modulus and high flexibility similar to elastomeric materials [44]. The EVA matrix shows a high compatibility with pores, making them an excellent candidate for incorporation of electrical macrodipoles [45].

In order to achieve the above-mentioned purpose, our prior studies have been performed on EVA porous piezoelectric polymers [46]. SEM analysis has been realized to determine the homogeneity of gas cells' distribution in the EVA matrix. A good distribution of cells/voids in the EVA matrix has been obtained for all fabricated films. Various means of increasing the intrinsic characteristics of the copolymers were also studied and demonstrated the simplicity and advantage of working in the pseudo-piezoelectric effect.

To continue in the same research area, the objective of this study is to evaluate the energy harvesting by EVA porous polymers in order to increase the conversion abilities of porous piezoelectric polymers. The goals of the next sections are to: (i) characterize mechanical and piezoelectric proprieties of these materials with their mechanical/thermal stability, and (ii) use a theoretical model and experimental setup to demonstrate the possibility of using the cellular EVA piezoelectric for mechanical energy harvesting applications.

2. Materials, Process, and Characterizations

2.1. Materials Preparation

The matrix material used in this study was a poly(ethylene-*co*-vinyl acetate) random copolymer (EVA, Greenflex® FC45F) supplied by ENI Versalis Spa (Milan, Italy). The EVA used has a vinyl acetate content of 14 wt.%. The cellular EVA films were produced by a melt-state coextrusion process using 0%, 1%, and 2% of Hydrocerol® ITP848 (Clariant, Muttenz, Switzerland) as a chemical foaming agent (CFA). The as-produced films had a thickness of around between 160 and 310 µm. You can find more information on film elaboration and morphological analysis in our previous work [46].

2.2. Electrical Charging/Ionization Process

To create piezoelectric properties in our porous polymer films, a high voltage was applied perpendicular to the material surface to charge the encapsulated gas in the foams (air) and create electrical macro-dipoles. To charge the porous copolymer samples, a high-resolution sputter coater coats the film with a silver electrode on both surfaces (12 nm thick) under high vacuum, and then subjects it to DC electric fields E of 10 kV/mm.

High voltage was delivered by a voltage amplifier of gain 1000 (TREK10/10 B, Trek Inc., Lisses, France). Input was controlled by a function generator (Agilent 33220A, Santa Clara, CA, USA). The sample had a surface area of 400 mm^2, and the electrical charges were injected for a duration of 15 min. Figure 1 gives a schematic representation of the electrical ionization process. The electrical charging process was performed in silicone oil. The silicone oil used in the experiment is a dielectric liquid consisting of polydimethylsiloxane with a purity specially controlled for use in electrical engineering.

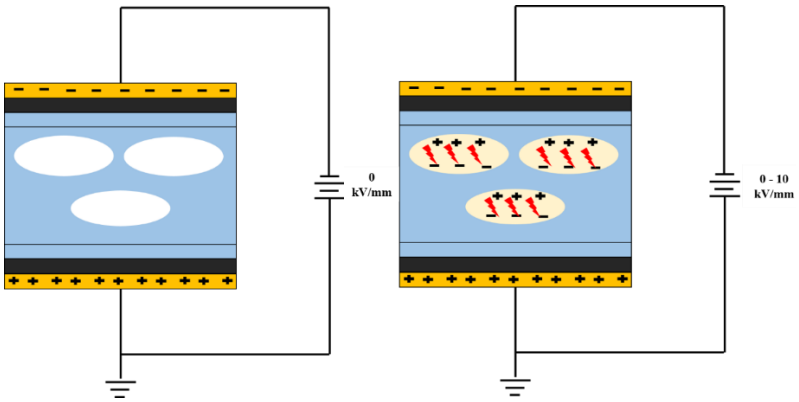


Figure 1. Illustration of electrical ionization process using DC generator.

2.3. Physical Characterizations

The porosity, foam, or void content of porous polymer materials is an important parameter that must be measured with a high precision balance (OHAUS® ADVENTURER™, NJ, USA) (m = 10^{-4} g). The porous films' Young's modulus was determined using a computer-controlled EM MODEL 00 UNIVERSAL testing machine (ERM-automatismes, Carpentras, France) with a 20 kN load cell [47].

The longitudinal piezoelectric coefficient of electrically ionized cellular EVA film is determined using a piezometer (model YE2730). A HP 4284A LCR meter was used to do the dielectric measurements (Agilent Technologies, Santa Clara, CA, USA).

2.4. Experimental Harvesting Energy Test

For the active energy harvesting system investigated within the scope of this study, electric energy parameters were performed. The setup for characterizing the current and voltage collected by flexible materials is shown schematically in Figure 2. These measurements were made with a one-degree-of-freedom table. The material is held in

place by two jaws, one of which is movable and attached to the table through a degree of freedom, while the other is immovable and connected to the force sensor.

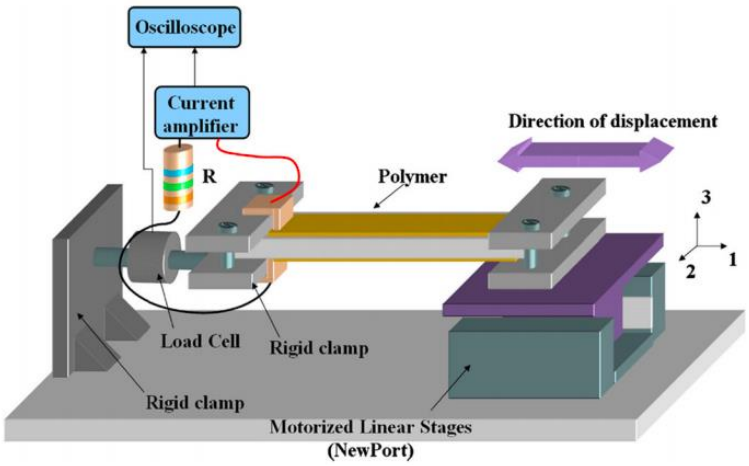


Figure 2. Schematic illustration of the experimental setup for the energy harvesting measurements.

The NewPort table was controlled using a computing process. It is possible to obtain a wide range of strain over a wide frequency band. At f_m = 4 Hz, the film was stretched with maximum transverse strain amplitudes of 0.25%, 0.50%, and 0.75%. The output from the current and voltage harvested by the piezoelectric materials were monitored using Stanford Model SR 570 (Stanford Research Systems Inc., Sunnyvale, CA, USA) and Scope Gw INSTEK GDS-2074A (INSTEK, New Taipei City, Taiwan), respectively.

3. Results and Discussions

3.1. Mechanical Characterization

The material used in this work is a thin film flexible multilayer structural device with an EVA film between 160 and 320 µm. The device is then encapsulated in between two thin EVA protective layers without pores. The multilayer material is sandwiched in between two 12 nm thin film metal electrodes (Figure 3). The film compositions are summarized in Table 1.

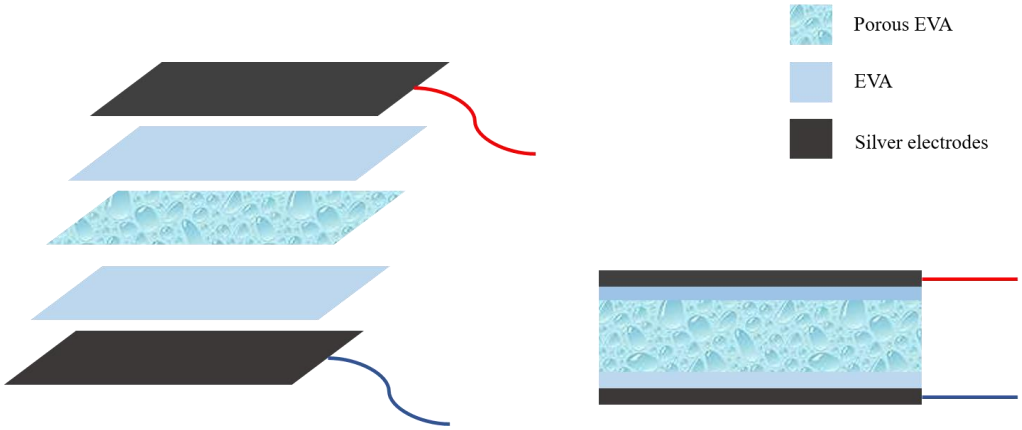


Figure 3. Description of the composition of pseudo-piezoelectric cellular EVA films. The mechanical tests' objective is to describe the macroscopic behavior of the three compositions studied in the static and dynamic case, then establish the relationship between this macroscopic and the microscopic material characteristics.

Table 1. Film compositions before and after extrusion operation.

Samples	Before Extrusion			After Extrusion	
	Ethylene (%)	Vinyl Acetate (%)	Hydrocerol (%)	Poly(Ethylene-*co*-Vinyl Acetate) (%)	Porosity (%)
EVA 0	86	14	0	100	0
EVA 1	85	14	1	63	37
EVA 2	84	14	2	35	65

The objective of the mechanical tests is to describe the macroscopic behavior of the three compositions studied in the static and dynamic case, then establish a relationship between these macroscopic and the microscopic material characteristics.

The Young's modulus according to the pourcentage of porosity was evaluated. The results presented in Figure 4 show that Young's modulus of the material decreases in the presence of porosity, as a typical result obtained with porous materials. The test was performed on four rectangular samples with a crosshead speed of 10 mm/min at room temperature.

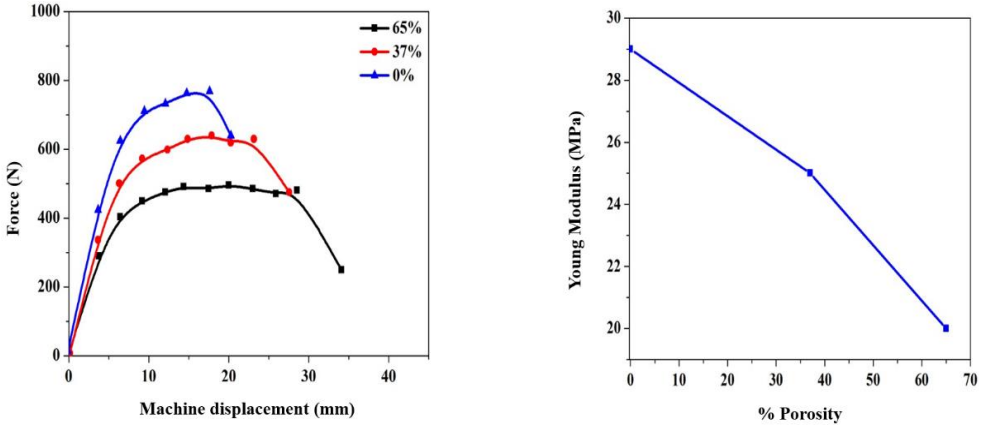


Figure 4. (**a**) Applied force as a function of machine displacement of EVA 0%, EVA 37% and EVA 65%. (**b**) Young's modulus as a function of porosity percentage.

Figure 4 reports the mechanical properties as a function of cellular morphology. It is clear that for EVA compositions, the values decrease linearly with pore content (about 29, 25 and 20 MPa for 0%, 37% and 65% of pores, respectively). For the same condition to each film, EVA 65% generates bigger strains than EVA 37% and EVA 0%. Raising the percentage of gas cells raises the quantity of mechanical energy absorbed by the materials, thus increasing the material flexibility. This flexibility is due to the shape and the gas cell number, which create sensitivity to the mechanical stress.

The cyclic mechanical loading at various frequencies is measured using the dynamic mechanical analysis technique (DMA). For testing, a porous EVA is placed into the DMA's tensile grips. The sample is then subjected to a predefined maximum tensile stress, which elongates the material. The material is returned to zero force at the end of one cycle. All of the experiments were carried out at room temperature (25 °C).

Figure 5a,b represent the stress–strain hysteretic response of porous EVA when exposed to frequencies of 4 and 20 Hz, respectively. Each frequency was subjected to six separate tests. The average of the six experiments is shown in Figure 5. When porous piezoelectric EVA is exposed to cyclic mechanical stress, it develops hysteretic behavior. Microstructural changes such as cell morphology, matrix mechanical proprieties, and other potential permanent microstructural changes such as cracking cause the hysteretic response under the mentioned loading conditions.

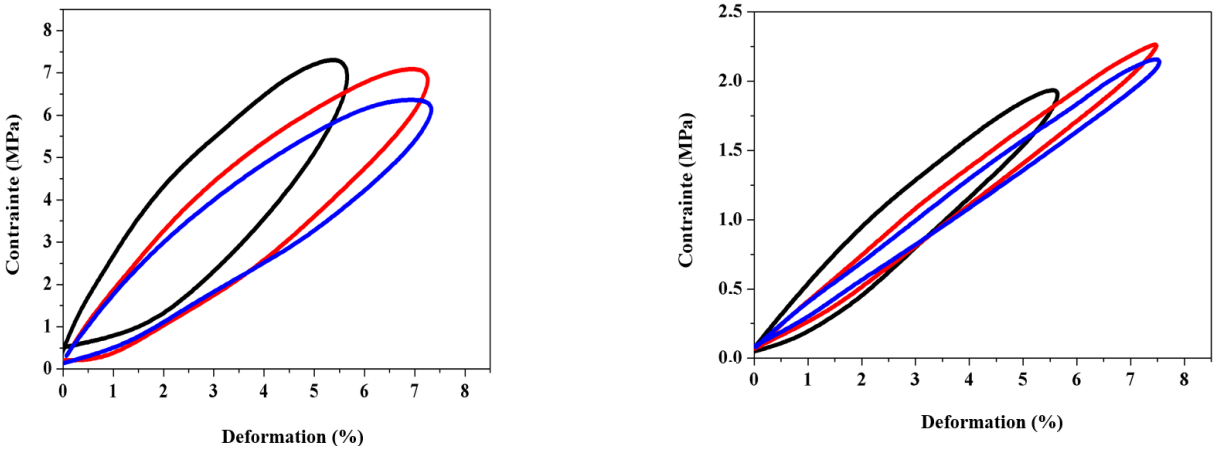


Figure 5. Stress–strain hysteretic response of EVA 0% (Black curve), EVA 37% (Red curve) and EVA 65% (Blue curve) with various cycles. (**a**) 4 Hz and (**b**) 20 Hz.

3.2. Influence of Environment Temperature and Time on the Piezoelectric Properties

The goal of this subsection is to test the piezoelectric properties' stability of the cellular EVA. The first experiment consists of measuring the piezoelectric constant as a function of the environmental temperature. The purpose of this experiment is to show the effect of temperature on the material. The first phase in the experiment was to apply a gradual temperature rise while maintaining constant pressure (5 MPa). The temperature was gradually raised from 0 to 180 °C, with a 20 °C increment every 10 min. The second experiment is to measure the piezoelectric constant as a function of time. The objective of this experiment is to show the capacity of the material to store electrical charges. An experimental measurement of the d_{33} piezoelectric coefficient as a function of time and temperature is shown in Figures 6 and 7. Figure 6 presents the changing of the piezoelectric constant with de-poling temperature for several silicone oil-ionized samples.

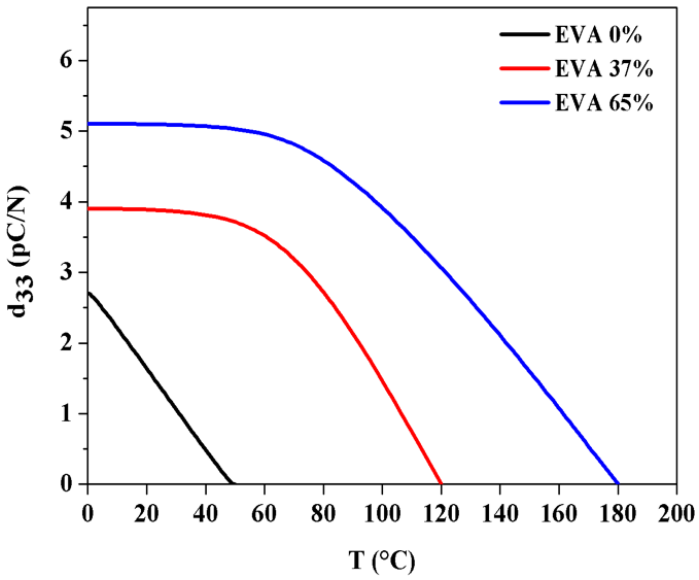


Figure 6. Piezoelectric coefficient as a function of depolarization temperatures charged in the silicone oil at room temperature.

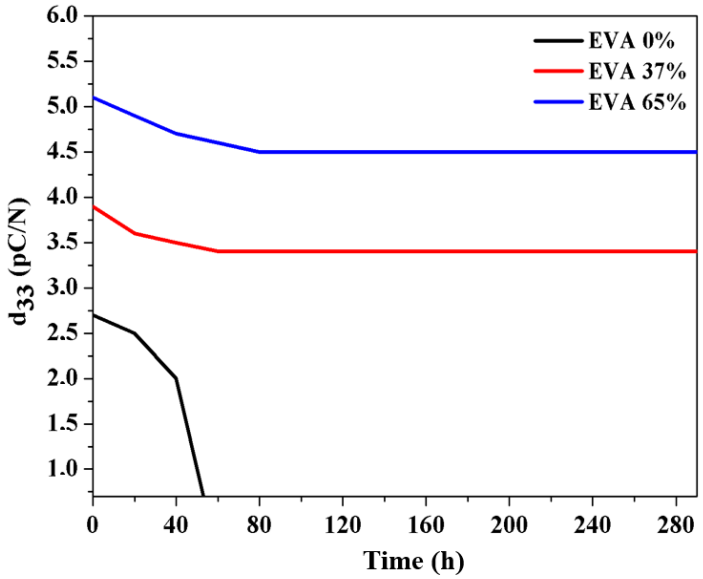


Figure 7. Piezoelectric coefficient as a function of time after ionization process charged in the silicone oil at room temperature.

The principal experimental results demonstrate that when temperature rises, the piezoelectric coefficient remains stable until it reaches a critical limit, at which point the piezoelectric constant reduces. The pores consolidate beyond this point, and the film loses its cells, as well as the local dipoles that provide the pseudo piezoelectric effect. The phase transition solid–liquid temperature is observed when the piezoelectric constant begins to decrease. Thermal depolarization shows a remarkable difference between a sample which contains charges in the defaults without pores (EVA 0%) and a sample which contains ionic dipoles with porous structure (EVA 37% and EVA 65%).

Figure 7 illustrates the temporal evolution of the piezoelectric coefficient, which was measured outside of the laboratory. After the relaxation period, the measurements were collected at room temperature. The d_{33} piezoelectric coefficient value for EVA 65% reduced from 5.1 to 4.5 pC/N from 0 to 65 h, after which it stabilized at 4.5 pC/N. However, these piezoelectric activities were unstable, and a reduction was observed 65 h after the ionization step. Moreover, the charge in cellular EVA remained constant after this time.

3.3. Energy Harvesting Study

3.3.1. Piezoelectric Harvested Current Model

The goal of modeling is to express the current harvested by a piezoelectric material in temporal domain. Modeling the effect of piezoelectric materials is written in the form of the following two fundamental equations. The piezoelectric constitutive equations of direct and converse effects are given below [14]:

$$S = s^E \times T + d_t \times E \tag{1}$$

$$D = d_t \times T + \varepsilon^T \times E \tag{2}$$

where S, T, D, E, ε^T, d and s^E are, respectively, the strain, the stress, the electric displacement, the electric field, the dielectric permittivity, the piezoelectric coefficient and the compliance.

It is possible to express the T stress as a function of strain S using Equation (1), given by:

$$T = \frac{S - d_t \times E}{s^E} \tag{3}$$

By substituting the expression of Equation (3) into Equation (2), the electrical displacement can be expressed as follows:

$$D = d_t \times \frac{S - d_t \times E}{s^E} + \varepsilon^T \times E \tag{4}$$

It is known that the expression of current harvested and electrical displacement is:

$$I = A \times \frac{\partial D}{\partial t} \tag{5}$$

A is the metalized surface of the polymer. Substituting Equations (4) into (5) gives:

$$I = A \times \left(\varepsilon^T - \frac{d_t^2}{s^E}\right) \frac{\partial E}{\partial t} + A \times \frac{d_t}{s^E} \frac{\partial S}{\partial t} \tag{6}$$

$\frac{\partial E}{\partial t}$ and $\frac{\partial S}{\partial t}$ are the time variation of the electrical field and strain as a function of time variation, respectively.

The electrical field output of the polymer across the load resistance is defined by the term:

$$E_R = -\frac{R \times I}{h} \tag{7}$$

where R the electrical resistance and h is the thickness of the polymer film.

The relation between Y material Young's modulus and the compliance is $Y = \frac{1}{s_{11}^E}$, so substituting Equation (7) into (6) gives:

$$I(t) = -A\left(\varepsilon^T - Yd_t^2\right)\frac{R}{h} \times \frac{\partial I}{\partial t} + A \times Yd_t \times \frac{\partial S}{\partial t} \tag{8}$$

Transforming Equation (8) into frequency domain, we can obtain the current I as:

$$I(p) = \frac{A \times Yd_t \times p}{1 + A\left(\varepsilon^T - Yd_t^2\right)\frac{R}{h} \times p} S(p) \tag{9}$$

Applying the transformation of inverse Laplace to Equation (9), we obtain the current harvested expression:

$$l^{-1}\{I(p)\} = I(t) = \frac{hYd_t}{\left(\varepsilon^T - Yd_t^2\right)R}\left(\gamma(t) - \frac{h}{A\left(\varepsilon^T - Yd_t^2\right)R} exp\left(-t\frac{h}{A\left(\varepsilon^T - Yd_t^2\right)R}\right)\right) S(t) \tag{10}$$

with the governing equation of mechanical motion being:

$$S(t) = S_M \sin(2\pi f_M \times t) \tag{11}$$

where S_M and f_M are maximum transverse strain and mechanical excitation frequency, respectively.

Substituting Equation (11) into (10), the current expression as a function of time and mechanical cycle excitation is expressed in the form:

$$I(t) = \frac{hYd_tS_M}{\left(\varepsilon^T - Yd_t^2\right)R}\left(\gamma(t) - \frac{h}{A\left(\varepsilon^T - Yd_t^2\right)R} exp\left(-t\frac{h}{A\left(\varepsilon^T - Yd_t^2\right)R}\right)\right) \sin(2\pi f_m \times t) \tag{12}$$

This harvested current depends on the level of mechanical strain, excitation frequency, material dimensions, electrical load and material proprieties. To validate this principle, an experimental study was performed. In order to predict output performances for charged porous films, the physical parameters of Equation (12) are presented in Table 2.

Table 2. Synthesis of materials' physical properties.

Material Proprieties	EVA 0%	EVA 37%	EVA 65%
Young Modulus (MPa)	29	25	20
Depolarization Temperature (°C)	74	67	61
Strain limit (%)	24	27	31
Piezoelectric Coefficient d_{33} (pC/N)	2.2	4.2	5.1
Time after deionization	30 h	33 days	59 days
Relative Permittivity	3.6	5.1	5.7

3.3.2. Energy Harvesting Results

During the energy harvesting studies, experimental measurements are taken to determine the electrical properties of porous EVA. To validate the proposed modeling approach provided in the preceding part, the three compositions are examined in order. More examples are provided to demonstrate the feasibility and usefulness of EVA porous piezoelectric polymers in the situation of complex mechanical conditions and realistic energy harvesting devices.

Figures 8–10 present the evolution of the electrical parameters (current and voltage harvested) as a function of time according to the applied strain using the three compositions of EVA. After analyzing the figures, it is clear that the electrical parameter increases by increasing the rate of deformation. For example, to obtain a value of the recovered current of 371 pA, it is necessary to apply a deformation of 0.75% in the case of EVA 0%; on the other hand, for porous structures (EVA 37%), it suffices to apply only 0.25%. For a strain of 0.75%, we can obtain a current of 320 pA by the EVA 0% instead of 1027 pA by the EVA 37% or 1692 pA by the EVA 65%. These results clearly show that increasing the porosity represents one of the best solutions for improving the electromechanical conversion of polymers in the pseudo piezoelectric mode.

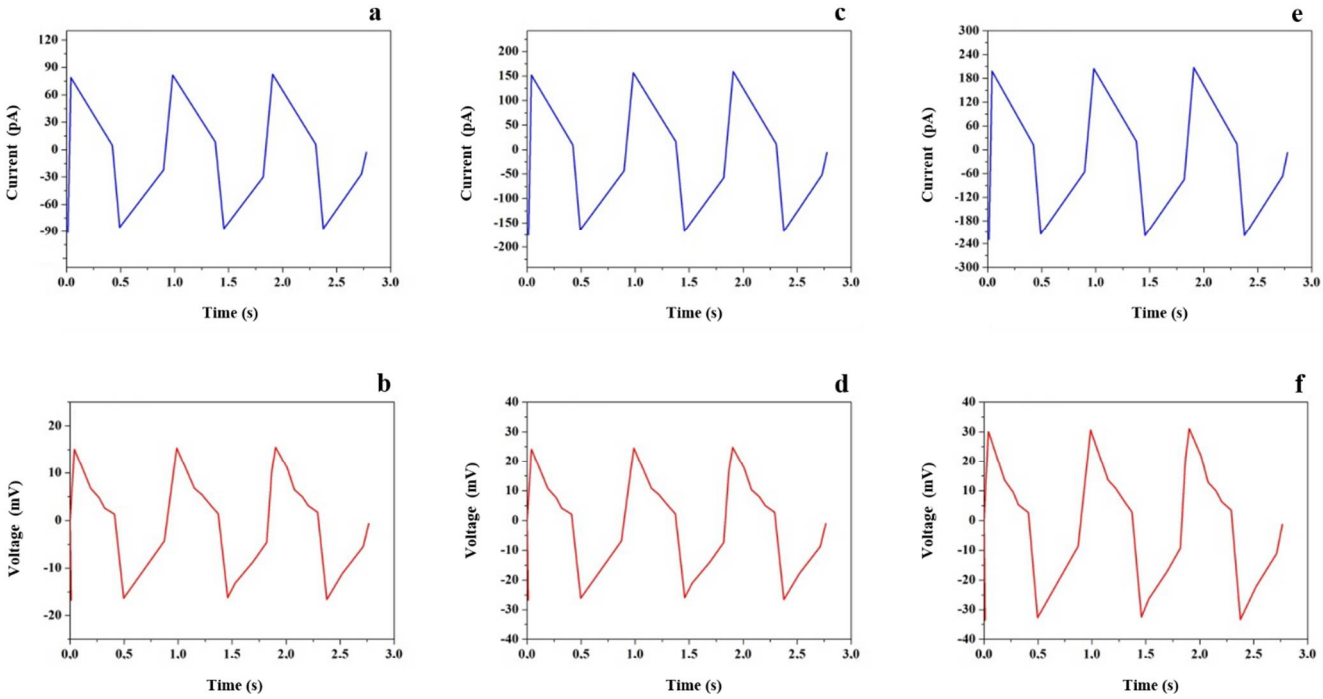


Figure 8. Electrical characteristics harvested by EVA 0% as a function of time under a transverse displacement with various values of strain S_M. (**a**) current harvested with S_M: 0.25%, (**b**) voltage harvested with S_M: 0.25%, (**c**) current harvested with S_M: 0.50%, (**d**) voltage harvested with S_M: 0.50%, (**e**) current harvested with S_M: 0.75%, (**f**) voltage harvested with S_M: 0.75%.

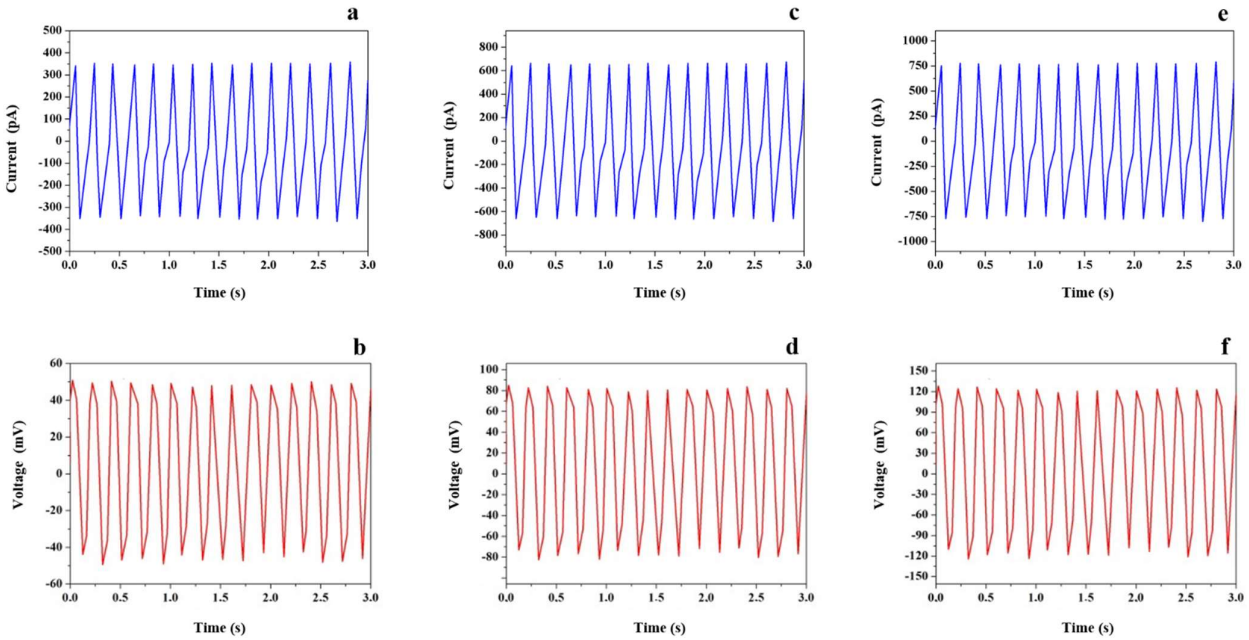


Figure 9. Electrical characteristics harvested by EVA 37% as a function of time under a transverse displacement with various values of strain S_M. (**a**) current harvested with S_M: 0.25%, (**b**) voltage harvested with S_M: 0.25%, (**c**) current harvested with S_M: 0.50%, (**d**) voltage harvested with S_M: 0.50%, (**e**) current harvested with S_M: 0.75%, (**f**) voltage harvested with S_M: 0.75%.

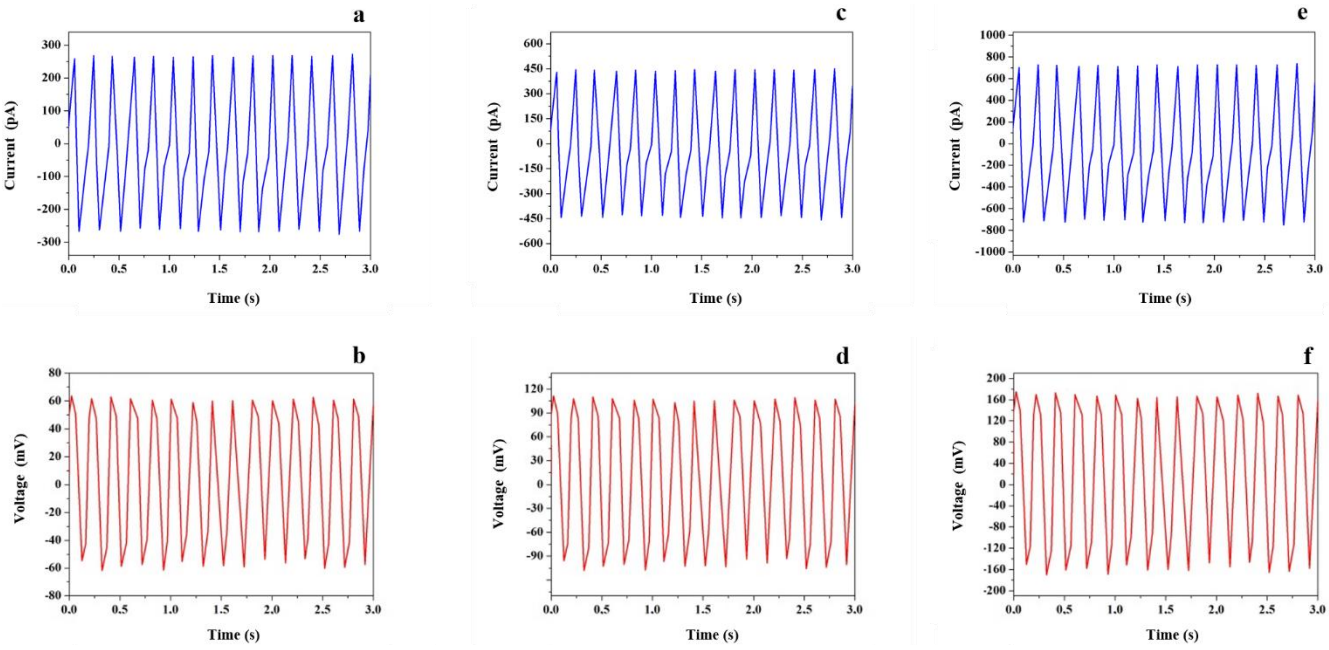


Figure 10. Electrical characteristics harvested by EVA 65% as a function of time under a transverse displacement with various values of strain S_M. (**a**) current harvested with S_M: 0.25%, (**b**) voltage harvested with S_M: 0.25%, (**c**) current harvested with S_M: 0.50%, (**d**) voltage harvested with S_M: 0.50%, (**e**) current harvested with S_M: 0.75%, (**f**) voltage harvested with S_M: 0.75%.

In the case of EVA 65%, the current delivered is well multiplied by a factor of 8 compared to EVA 0%. This suggests that the higher the porosity, the greater the current that can be harvested. The results obtained clearly show that increased strain has a remarkable influence on the voltage and current in the case of porous piezoelectric materials. The properties of the internal gas of porous films directly influence the electrical properties.

Figure 11 illustrates the dependence of current and voltage harvested using three compositions of porous EVA. The simulation behavior predicted by the proposed model

Equation (12) has been compared with the experimental setup of the power harvested by cellular polymers. In this figure, the points present the experimental results, and the curve presents the developed theoretical model.

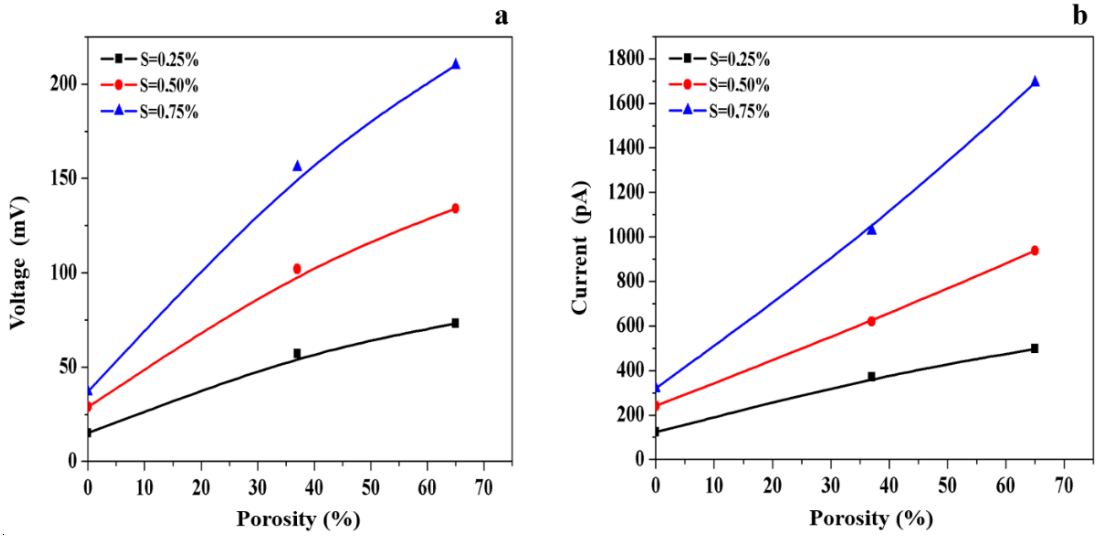


Figure 11. Porosity content influence on the electrical characteristics harvested by cellular EVA with three values of strain S_M: 0.25%, 0.50% and 0.75%. (**a**) Voltage harvested; (**b**) current harvested.

The values of 123, 241, and 320 pA were obtained, respectively, with 0.25%, 0.50%, and 0.75% of strain using EVA 0% at 4 Hz. In the case of EVA 37%, harvested current values at 4 Hz of 371, 620 and 1027 pA were obtained, respectively, with 0.25%, 0.50% and 0.75% of strain. For EVA 65%, harvested current values at 4 Hz of 497, 938 and 1692 pA were obtained, respectively, with 0.25%, 0.50% and 0.75% of strain.

Figure 11 shows a linear relationship between electrical properties and porosity. At the microscopic level, each cell is regarded as a generator containing a number of macro-dipoles. EVA 65% composition has more gas foams than EVA 37% composition. As a result, raising the proportion of space content in gas cells increases the number of macro-dipoles. For that, EVA 65% is a more sensible mechanical force compared to EVA 37% and EVA 0%. However, the increase in harvested current of the copolymer with an increase in the porosity that could be captured could be confirmed by the theoretical model with an error range between 0.3% and 5%. The harvested current significantly increases with increasing strain or porosity, achieving a high current value up to 1627 pA for EVA 65%. The same dependence is observed for the voltage harvested. These results demonstrate that porous materials are electrically and mechanically stable. As a result, it is evident that these porous polymers will be used in mechanical applications, particularly in the manufacture of energy harvesters and smart sensors based on vibration effect.

The results' analysis makes it possible to study the influence of the pores created in the polymer matrix. It also makes it possible to examine the dependence of these parameters on the mechanical applied stress and frequency range. This analysis was carried out with the aim of optimizing the operating interval for a better application in the field of sensor, actuation or vibratory energy harvesting.

4. Conclusions

This work presented the mechanical, physical, and morphological Poly(ethylene-*co*-vinyl acetate) (EVA) properties for different void concentrations. Additionally, the effect of porosity on the Young's modulus, piezoelectric coefficient, and the impact of physical properties of the co-polymer were analyzed.

Three different percentages of porosity were used to create and test porous piezoelectric polymers for energy harvesting. The theoretical model and experimental results were

found to be in good agreement. Various methods of improving the inherent properties of the polymers were also investigated, demonstrating the simplicity and usefulness of operating using pseudo-piezoelectric behavior. Porous piezoelectric polymers have been shown to possess significant mechanical energy that can be harvested. It can be concluded that the porosity has a significant effect on the mechanical proprieties of the piezoelectric porous polymers, and on the current, voltage and power in turn. Future research will focus on developing new systems and combining hybridization with other materials to improve the performance of harvested energy.

Author Contributions: Conceptualization, C.E., A.H., C.S., E.S., A.R., I.N. and M.R.; Data curation, C.E.; Formal analysis, C.S., A.R., E.M.L. (El Mehdi Laadissi) and E.M.L. (El Mehdi Loualid); Funding acquisition, A.H. and C.S.; Investigation, A.R. and I.N.; Methodology, A.H., C.S., E.M.L. (El Mehdi Laadissi) and A.E.B.; Project administration, A.H., A.E.B. and A.A.; Resources, C.E., E.S. and M.R.; Software, C.E., A.R., E.M.L. (El Mehdi Laadissi) and E.M.L. (El Mehdi Loualid); Supervision, A.H., A.E.B. and A.A.; Validation, C.S., I.N. and M.R.; Visualization, A.A.; Writing—original draft, C.E. and E.S.; Writing—review and editing, C.E., A.H. and C.S. All authors have read and agreed to the published version of the manuscript.

Funding: This research received no external funding.

Institutional Review Board Statement: Not applicable.

Informed Consent Statement: Not applicable.

Data Availability Statement: Not applicable.

Conflicts of Interest: The authors declare no conflict of interest.

References

1. Yang, L.; Chi, S.; Dong, S.; Yuan, F.; Wang, Z.; Lei, J.; Bao, L.; Xiang, J.; Wang, J. Preparation and characterization of a novel piezoelectric nanogenerator based on soluble and meltable copolyimide for harvesting mechanical energy. *Nano Energy* **2019**, *67*, 104220. [CrossRef]
2. Marwane, E.R. Lithium-ion battery modeling using equivalent circuit model. *Int. J. Eng. Appl. Phys.* **2021**, *1*, 48–60.
3. Jain, A.; Prashanth, K.J.; Sharma, A.K.; Jain, A.; Rashmi, P.N. Dielectric and piezoelectric properties of PVDF/PZT composites: A review. *Polym. Eng. Sci.* **2015**, *55*, 1589–1616. [CrossRef]
4. Zhang, Y.; Liu, X.; Wang, G.; Li, Y.; Zhang, S.; Wang, D.; Sun, H. Enhanced mechanical energy harvesting capability in sodium bismuth titanate based lead-free piezoelectric. *J. Alloy. Compd.* **2020**, *825*, 154020. [CrossRef]
5. Rjafallah, A.; Hajjaji, A.; Guyomar, D.; Kandoussi, K.; Belhora, F.; Boughaleb, Y. Modeling of polyurethane/lead zirconate titanate composites for vibration energy harvesting. *J. Compos. Mater.* **2018**, *53*, 613–623. [CrossRef]
6. Ennawaoui, C.; Lifi, H.; Hajjaji, A.; Elballouti, A.; Laasri, S.; Azim, A.-E. Mathematical modeling of mass spring's system: Hybrid speed bumps application for mechanical energy harvesting. *Eng. Solid Mech.* **2019**, *7*, 47–58. [CrossRef]
7. Ennawaoui, C.; Hajjaji, A.; Elballouti, A.; Azeddine, A.Z.I.M. Smart speed bump for mechanical energy harvesting from roads. *Int. J. Eng. Appl. Phys.* **2021**, *1*, 61–66.
8. Zhang, Y.; Bowen, C.R.; Ghosh, S.K.; Mandal, D.; Khanbareh, H.; Arafa, M.; Wan, C. Ferroelectret materials and devices for energy harvesting applications. *Nano Energy* **2018**, *57*, 118–140. [CrossRef]
9. Drozdov, A.D.; Christiansen, J.D.C. The effect of porosity on elastic moduli of polymer foams. *J. Appl. Polym. Sci.* **2019**, *137*, 48449. [CrossRef]
10. Lifi, H.; Ennawaoui, C.; Hajjaji, A.; Touhtouh, S.; Laasri, S.; Yessari, M.; Benjelloun, M. Sensors and energy harvesters based on (1–x)PMN-xPT piezoelectric ceramics. *Eur. Phys. J. Appl. Phys.* **2019**, *88*, 10901. [CrossRef]
11. Elhmamsy, Y.; Ennawaoui, C.; Hajjaji, A.; Boughaleb, Y. Theoretical study and Simulation method for optimizing the performance of advanced energy harvesting techniques. *Mater. Sci. Eng.* **2020**, *948*, 012014. [CrossRef]
12. Rjafallah, A.; Hajjaji, A.; Belhora, F.; Ballouti, A.; Touhtouh, S.; Guyomar, D.; Boughaleb, Y. PZT ceramic particles/polyurethane composites formalism for mechanical energy harvesting. *Eur. Phys. J. Appl. Phys.* **2020**, *89*, 30901. [CrossRef]
13. Qaiss, A.; Saidi, H.; Fassi-Fehri, O.; Bousmina, M. Porosity formation by biaxial stretching in polyolefin films filled with calcium carbonate particles. *J. Appl. Polym. Sci.* **2011**, *123*, 3425–3436. [CrossRef]
14. Rjafallah, A.; Hajjaji, A.; Belhora, F.; Guyomar, D.; Seveyrat, L.; EL Otmani, R.; Boughaleb, Y. Mechanical energy harvesting using polyurethane/lead zirconate titanate composites. *J. Compos. Mater.* **2017**, *52*, 1171–1182. [CrossRef]
15. Yang, K.; Rongong, J.A.; Worden, K. Damage detection in a laboratory wind turbine blade using techniques of ultrasonic NDT and SHM. *Strain* **2018**, *54*, e12290. [CrossRef]
16. Zhang, X.; Pondrom, P.; Sessler, G.M.; Ma, X. Ferroelectret nanogenerator with large transverse piezoelectric activity. *Nano Energy* **2018**, *50*, 52–61. [CrossRef]

17. Kachroudi, A.; Basrour, S.; Rufer, L.; Jomni, F. Air-spaced PDMS piezo-electret cantilevers for vibration energy harvesting. *J. Phys. Conf. Ser.* **2016**, *773*, 012072. [CrossRef]
18. Hanana, F.E.; Chimeni, D.Y.; Rodrigue, D. Morphology and mechanical properties of maple reinforced LLDPE produced by rotational moulding: Effect of fibre content and surface treatment. *Polym. Compos.* **2018**, *26*, 299–308. [CrossRef]
19. Wegener, M.; Gerhard-Multhaupt, R.; Bergweiler, S.; Wirges, W.; Pucher, A. Voided space-charge electrets? Piezoelectric transducer materials for electro-acoustic applications. In Proceedings of the Audio Engineering Society Convention 116, Berlin/Heidelberg, Germany, 8–11 May 2004.
20. Duc, C.; Stoclet, G.; Soulestin, J.; Samuel, C. Poly(ethylene oxide)/PEDOT: PSS blends: An efficient route to highly conductive thermoplastic materials for melt-state extrusion processing? *ACS Appl. Polym. Mater.* **2020**, *2*, 2366–2379. [CrossRef]
21. Cui, H.; Hensleigh, R.; Yao, D.; LoPinto, D.; Zheng, X. Three-dimensional printing of piezoelectric materials with designed anisotropy and their applications in underwater transducers. *Bull. Am. Phys. Soc.* **2020**, *65*, 1.
22. Mooney, D.; Baldwin, D.F.; Suh, N.P.; Vacanti, J.P.; Langer, R. Novel approach to fabricate porous sponges of poly(d,l-lactic-*co*-glycolic acid) without the use of organic solvents. *Biomaterials* **1996**, *17*, 1417–1422. [CrossRef]
23. Hmamsy, Y.; Ennawaoui, C.; Najihi, I.; Hajjaji, A. The synchronized electrical charge extraction regulator for harvesting energy using piezoelectric materials. In Proceedings of the International Conference on Digital Technologies and Applications, Fez, Morocco, 29–30 January 2021.
24. Schmidt, R.H.; Mosbach, K.; Haupt, K. A simple method for spin-coating molecularly imprinted polymer films of controlled thickness and porosity. *Adv. Mater.* **2004**, *16*, 719–722. [CrossRef]
25. Wegener, M.; Bauer, S. Microstorms in cellular polymers: A route to soft piezoelectric transducer materials with engineered macroscopic dipoles. *Chem. Phys. Chem.* **2005**, *6*, 1014–1025. [CrossRef] [PubMed]
26. Khan, T.; Acar, V.; Aydin, M.R.; Hülagü, B.; Akbulut, H.; Seydibeyoğlu, M. A review on recent advances in sandwich structures based on polyurethane foam cores. *Polym. Compos.* **2020**, *41*, 2355–2400. [CrossRef]
27. Qaiss, A.E.K.; Bousmina, M. Biaxial stretching of polymers using a novel and versatile stretching system. *Polym. Eng. Sci.* **2011**, *51*, 1347–1353. [CrossRef]
28. Wegener, M.; Bergweiler, S.; Wirges, W.; Pucher, A.; Tuncer, E.; Gerhard-Multhaupt, R. Piezoelectric two-layer stacks of cellular polypropylene ferroelectrets: Transducer response at audio and ultrasound frequencies. *IEEE Trans. Ultrason. Ferroelectr. Freq. Control.* **2005**, *52*, 1601–1607. [CrossRef]
29. Qaiss, A.; Saidi, H.; Fassi-Fehri, O.; Bousmina, M. Theoretical modeling and experiments on the piezoelectric coefficient in cellular polymer films. *Polym. Eng. Sci.* **2012**, *53*, 105–111. [CrossRef]
30. Bai, B.; Zhou, J.; Yin, M. A comprehensive review of polyacrylamide polymer gels for conformance control. *Pet. Explor. Dev.* **2015**, *42*, 525–532. [CrossRef]
31. Liu, T.; Peng, X.-F.; Mi, H.-Y.; Li, H.; Turng, L.-S.; Xu, B.-P. Preparation of fast-degrading poly(lactic acid)/soy protein concentrate biocomposite foams via supercritical CO_2 foaming. *Polym. Eng. Sci.* **2019**, *59*, 1753–1762. [CrossRef]
32. Handa, Y.P.; Zhang, Z. A new technique for measuring retrograde vitrification in polymer-gas systems and for making ultramicrocellular foams from the retrograde phase. *J. Polym. Sci.* **2000**, *38*, 716–725. [CrossRef]
33. Hmamsy, Y.; Ennawaoui, C.; Hajjaji, A. Study and design the circuit for piezoelectric vibration energy harvester to charge a datalogger. *Int. J. Eng. Appl. Phys.* **2021**, *1*, 18–25.
34. Neef, A.; Samuel, C.; Stoclet, G.; Rguiti, M.; Courtois, C.; Dubois, P.; Soulestin, J.; Raquez, J.-M. Processing of PVDF-based electroactive/ferroelectric films: Importance of PMMA and cooling rate from the melt state on the crystallization of PVDF beta-crystals. *Soft Matter* **2018**, *14*, 4591–4602. [CrossRef] [PubMed]
35. Ennawaoui, C.; Hajjaji, A.; Azim, A.; Boughaleb, Y. Theoretical modeling of power harvested by piezo-cellular polymers. *Mol. Cryst. Liq. Cryst.* **2016**, *628*, 49–54. [CrossRef]
36. Wirges, W.; Wegener, M.; Voronina, O.; Zirkel, L.; Gerhard-Multhaupt, R. Optimized preparation of elastically soft, highly piezoelectric, cellular ferroelectrets from nonvoided poly (ethylene terephthalate) films. *Adv. Funct. Mater.* **2007**, *17*, 324–329. [CrossRef]
37. Ma, N.; Yang, Y. Enhanced self-powered UV photoresponse of ferroelectric $BaTiO_3$ materials by pyroelectric effect. *Nano Energy* **2017**, *40*, 352–359. [CrossRef]
38. Yan, S.; Lu, J.; Song, W.; Xiao, R. Flexible triboelectric nanogenerator based on cost-effective thermoplastic polymeric nanofiber membranes for body-motion energy harvesting with high humidity-resistance. *Nano Energy* **2018**, *48*, 248–255. [CrossRef]
39. Mokhtari, F.; Shamshirsaz, M.; Latifi, M. Investigation of β phase formation in piezoelectric response of electrospun polyvinylidene fluoride nanofibers: LiCl additive and increasing fibers tension. *Polym. Eng. Sci.* **2015**, *56*, 61–70. [CrossRef]
40. Malki, Z.; Ennawaoui, C.; Hajjaji, A.; Najihi, I.; ElJouad, M.; Boughaleb, Y. Pedestrian crossing system for the mechanical energy harvesting using piezoelectric materials. *Mater. Sci. Eng.* **2020**, *948*, 012030. [CrossRef]
41. Pointner, T.; Wegener, M. Low voltage driven dielectric membrane actuators integrated into fast switching electronic circuit boards. *Smart Mater. Struct.* **2019**, *28*, 084002. [CrossRef]
42. Cao, Y.; Figueroa, J.; Pastrana, J.J.; Li, W.; Chen, Z.; Wang, Z.L.; Sepúlveda, N. Flexible ferroelectret polymer for self-powering devices and energy storage systems. *ACS Appl. Mater. Interfaces* **2019**, *11*, 17400–17409. [CrossRef]
43. Hamdi, O.; Mighri, F.; Rodrigue, D. Piezoelectric property improvement of polyethylene ferroelectrets using postprocessing thermal-pressure treatment. *Polym. Adv. Technol.* **2018**, *30*, 153–161. [CrossRef]

44. Wu, W.; Kurup, S.N.; Ellingford, C.; Li, J.; Wan, C. Coupling dynamic covalent bonds and ionic crosslinking network to promote shape memory properties of ethylene-vinyl acetate copolymers. *Polymers* **2020**, *12*, 983. [CrossRef] [PubMed]
45. Allan, J.M.; Mumin, A.; Wood, J.A.; Xu, W.Z.; Wu, W.; Charpentier, P.A. Silica aerogel-poly(ethylene-*co*-vinyl acetate) composite for transparent heat retention films. *J. Polym. Sci.* **2014**, *52*, 927–935. [CrossRef]
46. Ennawaoui, C.; Lifi, H.; Hajjaji, A.; Samuel, C.; Rguiti, M.; Touhtouh, S.; Courtois, C. Dielectric and mechanical optimization properties of porous poly (ethylene-*co*-vinyl acetate) copolymer films for pseudo-piezoelectric effect. *Polym. Eng. Sci.* **2019**, *59*, 1455–1461. [CrossRef]
47. Kanzaoui, M.; Ennawaoui, C.; Eladaoui, S.; Hajjaji, A.; Guenbour, A.; Boussen, R. Study of the physical behavior of a new composite material based on fly ash from the combustion of coal in an ultra-supercritical thermal power plant. *J. Compos. Sci.* **2021**, *5*, 151. [CrossRef]